In Vivo Bone Engineering in a Rabbit Femur

Jeffrey A. Fialkov, MD, MSc, FRCS(C)*
Chantal E. Holy, PhD†
Molly S. Shoichet, PhD†
John E. Davies, BDS, PhD, DSc†‡

Toronto, Ontario, Canada

The repair of bone defects in reconstructive surgery has significant limitations. Donor site morbidity, limited supply of autograft, and risks and complications associated with allografting and synthetic bone substitutes are among the most significant. In an effort to address these problems, the search for an ideal bone replacement has led to the development of a new method of poly(lactide-*co*-glycolide) (PLGA) foam processing, enabling the production of a biodegradable scaffold with similar porosity to human trabecular bone. In this study, these scaffolds were evaluated for bone repair in vivo in a femoral critical-sized segmental defect in New Zealand White (NZW) rabbits. Three groups of nine animals were investigated. In the first group, the critical-sized defects were empty. Scaffolds alone were implanted in the second group, whereas autologous bone marrow cell-loaded scaffolds were implanted in the third group. Animals ambulated freely for 8 weeks after surgery, and bone formation throughout the defects was serially assessed radiographically and quantified using a bone formation index (BFI) measure. Postmortem radiography and histology were also undertaken to examine bone formation. There was a significant effect of applying this technology to the amount of bone formed in the defects as determined by the BFI ($F = 3.41$, $P < 0.05$). The mean BFI for the cell-loaded scaffolds was greater than for the control group at all measured time points (2-, 4-, 6-, and 8-week radiographs). This difference was significant for the 2- and 8-week radiographs ($P < 0.05$). Qualitative histological assessment confirmed these findings. We concluded from these findings that these PLGA scaffolds loaded with marrow-derived progenitor cells yield significant bone formation in a critical-sized rabbit femoral defect. This technology comprising a novel scaffold design and autologous cells may provide an alternative to current strategies for reconstruction of bony defects.

Key Words: Tissue engineering, PLGA scaffold, marrow cells, bone, critical sized defect, rabbit femur, bone formation index

The repair of bone defects in plastic and orthopedic surgery continues to pose a number of clinical problems. Although autologous bone has been the historical standard for these procedures as a source of reconstructive material, it has significant limitations. In particular, donor site morbidity, including pain, loss of function, and local injury in the harvesting procedure, and a limited supply of bone are among the most significant of these. The use of allograft also carries with it significant problems, including disease transmission, host rejection, and lack of osteoinductive properties.[1]

In an effort to address these problems, the search for an ideal material has led to the development of several reconstructive options to engineer new bone tissue. These include synthetic osteoconductive bone substitutes and osteoinductive compounds such as bone morphogenetic protein or demineralized bone powder[2–6] and, more recently, osteoinductive calcium phosphate materials.[7] The development of synthetic resorbable scaffolds of either inorganic or polymer composition[8,9] as carriers of progenitor cells of various tissues has facilitated the move toward this ideal material.[10,11] Furthermore, the ability to expand potentially osteogenic bone marrow–derived mesenchymal stem cells by cell culture has enabled the loading of such scaffolds with bone progenitor cells for in vivo implanta-

From the *Department of Surgery, Division of Plastic Surgery, Sunnybrook and Women's College Health Sciences Center, †Institute of Biomaterials and Biomedical Engineering, and Department of Chemical Engineering and Applied Chemistry, Faculty of Applied Science and Engineering, and ‡Faculty of Dentistry, University of Toronto, Toronto, Ontario, Canada.

Address correspondence to Dr Fialkov, Sunnybrook and Women's College Health Sciences Center, 2075 Bayview Avenue, M1-519A, Toronto, Ontario, Canada M4N 3M5; e-mail: Jeff.Fialkov@swchsc.on.ca

tion.[12,13] Although various cell-based strategies for bone tissue engineering have been extensively reviewed elsewhere,[14–17] these and other studies have also illustrated several issues that have still to be addressed in scaffold design. For example, some calcium phosphate scaffolds demonstrate a limited ability to degrade in vivo,[18] whereas others degrade too rapidly in the presence of explanted marrow.[19] Furthermore, both inorganic[12] and organic[20] scaffolds have been used whose geometries preclude invasion by bone cells and tissue. Nevertheless, some inorganic and organic biodegradable scaffolds have been shown to permit tissue invasion[21] and result in bony union of critical-sized defects and restoration of function after seeding with either autologous marrow-derived cells in ruminants[19] and lagomorphs[22] or bovine cells in athymic mice.[23]

Such cell-based scaffolding strategies for bone engineering should, from a practical therapeutic standpoint, rely on autologous cells and degradable scaffold materials. Thus, although previous work has demonstrated the feasibility of various aspects of such an approach, a complete strategy has yet to be adequately demonstrated in a clinically applicable and reproducible manner.

The current limitations of these approaches are related to the architecture and composition of the implantable constructs themselves, which should allow a three-dimensional distribution of cells in vitro, thereby accelerating bone healing in vivo. For example, scaffold macroporosity has been known to be a critical factor in cell migration and bone matrix elaboration in vitro,[24] but pore bridging and occlusion of scaffold pores by cells have been shown to occur with both inorganic[21,25,26] and organic[20,27] scaffold materials. We have also shown that this problem can be avoided by increasing the nominal macropore size.[21,22,28,29] The size and number of interconnecting channels within the scaffolds are also important.[30] Kadiyala et al[12] showed that bone grew preferentially along the implant/host interface but not throughout the bulk material of macroporous scaffolds exhibiting no macroporous interconnectivity. Similarly, Ishaug-Riley et al[20] found that, with poly(lactide-*co*-glycolide) (PLGA) foams of 300- to 500-μm pore size, bone cells and tissue were only found within 300 μm of the outer edge of the scaffold, which inhibited cell growth and survival below the first pore layer.

A new method of PLGA 75:25 production developed in our laboratory has overcome this obstacle as demonstrated in vitro.[28,31] The new processing route enables the production of a biodegradable scaffold with similar porosity to that found in human trabecular bone, facilitates the formation of bone throughout the scaffold, and thus overcomes previous geometrical limitations. Moreover, in vitro studies indicate that the rate of degradation of this scaffold is slower than that of bone formation in vivo, suggesting its applicability in vivo.[32] The combination of mesenchymal stem cell isolation and expansion methods together with this new method of PLGA scaffold production seems to be a promising solution to the problems thus far encountered.

Therefore, in the current study, PLGA scaffolds were evaluated for bone repair in vivo in a femoral critical-sized segmental defect in New Zealand White (NZW) rabbits. For this study, three groups of nine animals were investigated. In the first group, the critical-sized defects were left empty. Scaffolds alone were implanted in critical-sized femoral defects of the second animal group, whereas expanded autologous bone marrow cells were loaded onto the scaffolds implanted in the third group. Animals were allowed to ambulate freely for 8 weeks after surgery, and bone formation throughout the defects was assessed radiographically every 2 weeks using a novel radiographic density measurement method that we have called the bone formation index (BFI). Postmortem radiography and histology were undertaken to examine new bone within the defects.

Materials and Methods

Animal Model

The NZW rabbit model for a nonhealing (critical-sized) defect of the femur has been previously established.[3,33] Based on these studies and our pilot study, we used the following model: NZW rabbits with a unilateral femoral osteotomy gap of 1.2 cm created surgically under general anesthetic and stabilized by a 2.7-mm mandibular reconstruction plate fixated with three screws on either side of the osteotomy site. Three treatment groups (nine rabbits per group) were compared for quantity of bone formation by the BFI.

Animal Population and Group Allocation

A total of 27 female NZW rabbits (Riemans Fur Ranches Limited, St. Agatha, Ontario, Canada) were entered into the study. The weight of all rabbits ranged from 2.0 to 2.5 kg before surgery (no statistical differences were seen in the increases in weight between animals at sacrifice). The animals were housed in individual cages at the Sunnybrook Health Science Centre Animal Research Facility and were cared for in accordance with Canadian Council on

Animal Care Guidelines. All rabbits underwent a 1-week quarantine period before commencing the experiment, during which they were screened to exclude acute and chronic medical conditions. All animals were provided with food (Shur-Gain, St. Mary's, Ontario, Canada) and water ad libitum. Animals that developed any signs of illness or those requiring medication during the holding period were excluded from the study. An overnight (14-hour) food and water deprivation period preceded all general anesthetic procedures. Rabbits were randomly assigned to one of three treatment groups: I, II, and III. Two animals died during surgery, and another was excluded as a result of infection. These animals were replaced in the study to maintain the individual group size (n = 9).

Scaffold Processing

Poly(DL-lactic-co-glycolic acid) scaffolds were prepared as previously described.[28] Briefly, glucose crystals were dispersed in a PLGA 75/25 solution in dimethylsulfoxide (BDH, Toronto, Ontario, Canada). The polymer was precipitated, and the glucose crystals were extracted in water from the precipitated polymer. Scaffolds were dried to constant mass (0.01 mm Hg, 72 hours) before use. The scaffolds were cylindrical in shape, with a diameter of 1 cm and length of 1.2 cm. Scaffolds were sterilized using an argon gas radiofrequency glow discharge plasma sterilization procedure at 100 W for 4 minutes. Scaffolds for cell culture were permeabilized with 70% ethanol for 10 minutes, washed in α-minimum essential medium (MEM) three times, and then seeded with cells (see below).

Bone Marrow Harvest

Rabbits from all three groups (n = 27) underwent bone marrow aspiration from bilateral iliac crests. Two weeks before the scheduled date for the osteotomy and after a 1-week holding period, aspirates were isolated and cultured as described below. The rabbits were anesthetized with Ketamine (ketamine hydrochloride, 50 mg/kg), Rompun (xylazine, 5 mg/kg) and acetylpromazine (0.75 mg/kg) by means of intramuscular induction and mask inhalation (2%–4% halothane volatilized with O_2) for maintenance. The iliac crest sites were prepared with 1% povidone iodine solution, and an 18-gauge spinal needle was introduced into the dorsal iliac spine. The trochar was removed from the needle, and a syringe containing 3 ml heparin solution (1,000 U/ml) was attached to the hub. A total of 3 ml marrow was aspirated from each ilium (6 ml per rabbit).

Culture Technique and Isolation of Osteoprogenitor Cells

Group III marrow aspirates were diluted with phosphate-buffered saline and passed through a 100-μm cell strainer. The resultant suspension was layered on a Ficoll gradient run at 1,400*g* to isolate further the nucleated marrow cells. This cell suspension was placed into a fully supplemented medium: α-MEM supplemented with 15% fetal bovine serum, 50 mg/ml ascorbic acid, 10 mM β-glycerophosphate, 10^{-8} M dexamethasone, and antibiotics (0.1 mg/ml penicillin G, 0.05 mg/ml gentamicin, and 0.3 mg/ml Fungizone).[34,35] These primary bone marrow–derived cells were seeded on PLGA 75:25 1-cm^3 cylindrical scaffolds as follows. Cells were maintained in culture for 6 days with medium changes at days 2 and 5. On day 6, cells were trypsinized (0.01% and 10 mM EDTA in phosphate-buffered saline) and seeded on separate prewetted scaffolds at a concentration of 7.5×10^5 cells/cm^3. The culture medium was changed at days 10, 12, and 15, and after 15 days, each of the nine cell-loaded scaffolds was delivered to the Animal Research Facility at Sunnybrook Health Science Center for implantation in the Group III rabbits.

Operative Procedure

All 27 rabbits underwent the following operative procedure. An induction mixture of Ketamine (ketamine hydrochloride, 50 mg/kg), Rompun (xylazine, 5 mg/kg), and acetylpromazine (0.75 mg/kg) was administered intramuscularly, followed by a maintenance inhalational anesthesia of 2% to 4% halothane volatilized with O_2 and delivered by snout mask administered by a qualified veterinary technician.

The lateral left hind limb of each rabbit was shaved and prepared with antiseptic solution (10% povidone iodine) and sterile draped with the rabbit in the right lateral decubitus position. The left femur was exposed through a lateral longitudinal incision. The quadriceps muscles were retracted, and the entire femoral diaphysis was exposed. The periosteum was stripped from the bone using a periosteal elevator. A 2.7-mm titanium eight-hole linear reconstruction plate (mandibular, Leibinger) was then applied to the anterolateral cortex and fixated with six 2.7-mm diameter bicortical screws, with three on either side of the proposed osteotomy site. A reciprocating saw was then used to resect a 1.2-cm long segment of central diaphysis under saline irrigation. This size of defect was used, because our preliminary studies (unpublished) showed that a 1-cm defect, as has been

reported in the literature, was not a nonunion model. In all animals operated on, the femoral periosteum was stripped for a distance of 0.5 cm on either side of the osteotomy. No marrow extirpation was undertaken.

The osteotomy site was left unfilled in the nine control rabbits (Group 1) or filled with the cell-free PLGA scaffold in nine rabbits (Group II) and cell-seeded with PLGA scaffolds in a further nine rabbits (Group III). The incision was closed in two layers, and the rabbits were returned to a padded crib with oxygen delivery by mask until spontaneous and purposeful movement was noted.

Radiologic Analysis

Rabbits underwent standardized serial radiography of the osteotomized femurs immediately after surgery and at 2, 4, 6, and at 8 weeks. All radiographs were size standardized. To quantify the information on rate of bone formation available in these serial radiographs and to eliminate the variation in radiodensity between radiographs, a novel measure of bone quantity based on radiopaque area and radiodensity within the osteotomy defect was devised. We call this measure the BFI. Measurements of radiodensity and area were made using the ChemiImager 5500 Imaging System and photodensity analysis program (version 2.02; Alpha Innotech Corporation, San Leandro, CA).

Bone Formation Index

The BFI is defined as:

$$BFI_y = {}_{(N=1...n)} \{I_N/I_X \times A_N/A_y\}$$

where BFI_y is the BFI in the osteotomy gap area y, $_N$ represents the individual radiopaque regions numbered 1,2,3… that are visible in the osteotomy gap, I_N is the average radiodensity of the radiopaque region "N" within the osteotomy site, I_x is the average radiodensity of the intercortical (between cortices) space of the diaphyseal bone adjacent and proximal to the osteotomy site (chosen to represent the radiopaque value of bone unaffected by the presence of the osteotomy), A_N is the average area of the radiopaque region "N" within the osteotomy site, and A_y is the average area of the osteotomy gap measured from the proximal cortical edge to the distal cortical edge.

Postmortem Preparation and Analysis

In the eighth postoperative week, the animals were sedated by intramuscular injection of Rogarsetic (40 mg/kg) and Rompun (5 mg/kg) and euthanized with an intravenous infusion of 2 ml per 4.5-kg dose of Euthanyl containing 240 mg pentobarbital per milliliter. After sacrifice, the left femur was harvested and fixed in 10% buffered formalin.

Fixed bone samples were dehydrated in graded ethanol and embedded in Osteobed bone-embedding medium. The specimens were then cut longitudinally through the middle of the fixation plate. Each hemiblock so produced was prepared for microscopic observation. One hemiblock was polished, stained with van Gieson and Toluidine blue dyes, and mounted on a glass slide. This section was photographed to provide the histological images of the specimens. The other hemiblock was also polished (to 1 μm diamond paste) and sputter coated with platinum for examination by backscattered electron imaging in the scanning electron microscope. Images of individual fields of view were captured digitally (about 20 per sample to include the whole osteotomy site) and digitally combined into montages to illustrate the whole block face.

Statistical Analysis

ANOVA was used to analyze the effect of treatment (none versus alone versus loaded with marrow-derived cells) and time (2 versus 4 versus 6 versus 8 weeks) on the BFI. Tukey's Studentized range test was used to compare the BFI between treatment groups for the four time points.

Results

As mentioned previously, three animals were replaced in this study, which ensured the maintenance of the group size (n = 9) for each treatment group. All animals recovered rapidly and were freely ambulating after surgery; none experienced mechanical failure. Because all animals were killed after surgery at one time point (8 weeks), the serial radiographs provided the only means of observing the progress of healing at the operative site, whereas further radiographic and histological examination of the dissected femora was conducted postmortem. Because restoration of natural locomotor function after osteotomy would rely on bony union across the operative site, union was assessed postmortem using both radiographic and histological (light and backscattered electron photomicrographs). Thus, for each animal, union was scored (union = 1, nonunion = 0) independently by four examiners for each set of data, where for each examination method, the maximum union score would be 36 (nine animals per group, four examiners). The results of these postmortem ex-

aminations are summarized in Figure 1, where the maximum union score is normalized to 1 (nonunion = 0). These results clearly demonstrated that the visual postmortem assessment score depended on the type of data being examined, with radiographs providing generally high scores and light micrography providing the lowest scores. Given the obvious limitations associated with two-dimensional analyses of three-dimensional healing (light and electron microscopy), we demonstrated that it was possible to prove union by changing the plane of examination as is shown in Figure 2. Nevertheless, our results showed that by the termination of the experimental period (8 weeks), there were no visually evident differences between union rates in Groups II and III, although Group I animals (controls) exhibited less union.

Contrary to the postmortem results described previously, the serial radiographs obtained after surgery and at 2, 4, and 6 weeks revealed obvious visual differences between experimental groups. We quantified these differences by establishing the BFI measurement as described previously. An example of the measurement technique is illustrated in Figure 3. ANOVA revealed an overall significant treatment effect on the BFI ($F = 3.41$, $P < 0.05$) together with an overall effect of time that demonstrated a significant increase in BFI for all groups ($F = 23.64$, $P < 0.0001$). Specifically, these analyses demonstrated that there was no significant difference between the mean BFI for Groups II and III (scaffold only [an example of the scaffold geometry is shown in Figure 4] and scaffold plus cells, respectively) at 8 weeks, confirming the visual examination of postmortem data. Nevertheless, these means (at 8 weeks) were significantly greater than in the control group. Indeed, the mean BFIs for the cell-loaded scaffolds (Group III) were greater than for the control group at all measured time points (2, 4, 6, and 8 weeks). This difference was significant for the 2- and 8-week radiographs ($P < 0.05$). The mean BFI for the cell-free scaffold group (Group II) was greater than for the control group (Group I, empty defect) at all time points, although this was only significant at 8 weeks. The quantitative results of BFI for each treatment group over time are illustrated in Figure 5.

Qualitative assessment of histologic, radiographic, and backscattered electron images revealed an unexpected but consistent pattern in the gross morphology of the newly formed bone, which seemed to remodel over the survival period, demonstrating a trend of resorption adjacent to the fixation plate and bony deposition on the opposing side of the defect, as shown in Figure 6. In addition, all animals showed significant quantities of subperiosteal bone formed on the opposing side of the femur to the fixation plate. From the serial radiographs, it was clear that this bone started to form in the distal subperiosteal region immediately proximal to the knee and therefore distant from the osteotomy site. This bone, which appeared on radiographs as a bony spicule, grew with time to extend outside the osteotomy site toward the proximal end of the femur and occasionally united with the proximal femoral shaft. This neocortex formed at a distance of approximately the width of the natural femur on the side opposing the fixation plate and was observed in all experimental groups but not in all rabbits. Both the quantitative results (BFI) and qualitative assessments (postmortem examination) confirmed that a greater quantity of bone formed at earlier time points in the scaffold-containing groups (II and III), particularly in the cell-containing group (III).

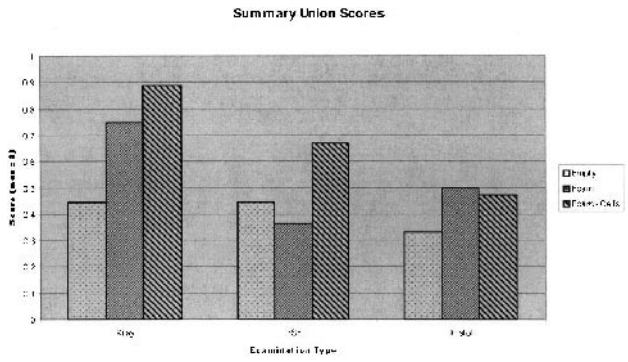

Fig 1 Summary of union scores assessed by radiographic, histologic, and backscattered electron imaging forms of examination.

Discussion

In vivo evaluation of the bone formation potential of tissue-engineered constructs was performed in three groups of nine animals, where bone formation in 1) empty defect, 2) scaffold-filled defect, and 3) cell-loaded scaffold-filled defect was compared. Although most radiographic data and all histological data were harvested postmortem, the results showed that there were no significant differences between the use of the scaffold alone (Group II) and the cell-seeded scaffolds (Group III). Although both Groups II and III exhibited more union and a statistically significantly greater volume of bone in defects at 8 weeks compared with control, by this time point, there was no advantage of employing the cell-seeding strategy. On the contrary, the serial radiographic evidence clearly showed that the volume of

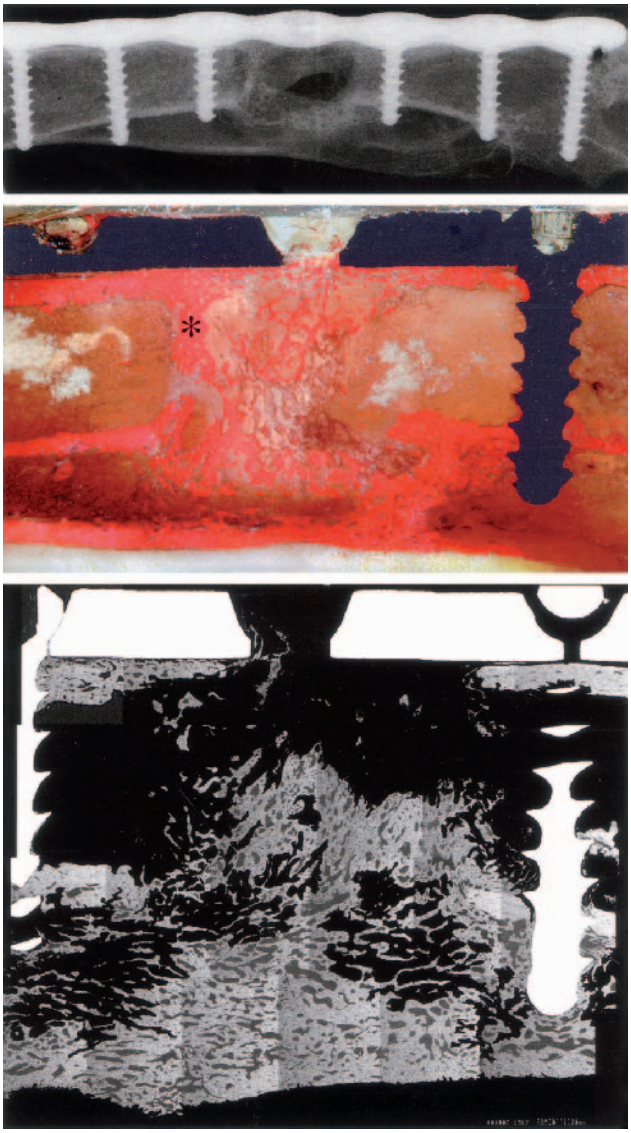

Fig 2 (Top) Radiograph of dissected specimen from Group III illustrating the degree of new bone formation both within and medial (below) to osteotomy site. The fixation plate is seen above and represents the lateral anatomical aspect. Note that the neocortex is visible immediately proximal to the knee (left) and extends proximal to the osteotomy site, which is almost obliterated by new bone formation. (Middle) Block face histological view of a hemisectioned specimen from Group III. Again, the neocortex is clearly seen, but the trabecular bone growth within the osteotomy site is also clearly visible and is being formed on the residue of the implanted foam, which has been lost during processing for histology (bone stained red is marked with *). (Bottom) A montage of backscattered electron images of a hemisection of another Group III specimen. This means of examination provides a clearer indication of the bone ingrowth into the surgical site. Bony union is evident in these specimens by each form of examination.

bone growth in the defect at the earliest postoperative time point examined (2 weeks) was greater in Group III animals than in either Group II or Group I animals, indicating an acceleration of healing of the defect at this early time point. Since the strategy of use for cell-seeded biodegradable scaffolds in bone tissue engineering is to allow regeneration of bone within the wound site, the acceleration of early healing is an important finding. To more thoroughly examine these earlier time points would require an additional and focused study, however. Indeed, without cell labeling and proof of functional phenotype, we are unable, with this histology-based study, to unequivocally state that the seeded cells were osteogenic or whether their presence provided a stimulus for growth through the release of biologically active mediators. Furthermore, the study protocol using undecalcified ground sections did not allow us to assess the degree of scaffold resorption.

Our observations were quantitatively based on a measure of bone formation that we referred to as the BFI. Other methods of bone quantification have been reported in the literature, although each has the potential for misinterpretation. Although bony union is the ultimate clinical goal of any nonhealing bone defect, its evaluation in vivo and postmortem is limited by the restrictions of any two-dimensional analysis, as shown in our union scores and postmortem histology. By devising the BFI, we have combined the factors of area and relative radiodensity within a bone defect to quantify the amount of bone formed within the area of interest. In this way, we have minimized the potential for "overreading" or "underreading" radiographs. If, for instance, two small spicules of bone are superimposed on a radiograph, suggesting there is bony union when, in fact, there is not, the effect on the BFI of relatively dense-appearing bone that results from this superimposition is reduced because of the small area involved. Furthermore, the measurement of defect bone volume (as opposed to bony union alone) has a significant role in tissue engineering, in that bone of a significant quantity is often needed in the clinical setting for which this technology is most applicable. From these results, we conclude that tissue-engineered bone using a bioresorbable scaffold strategy can yield a significant quantity of bone in a critical-sized segmental osteotomy in the rabbit femur. Although the mean BFI for the cell-loaded group was greater than for the control group at all periods, it was not found to be significant at 4 and 6 weeks. This is likely a result of an inadequate sample size for these groups, because the trend over time clearly shows the effect of treatment with the scaffold,

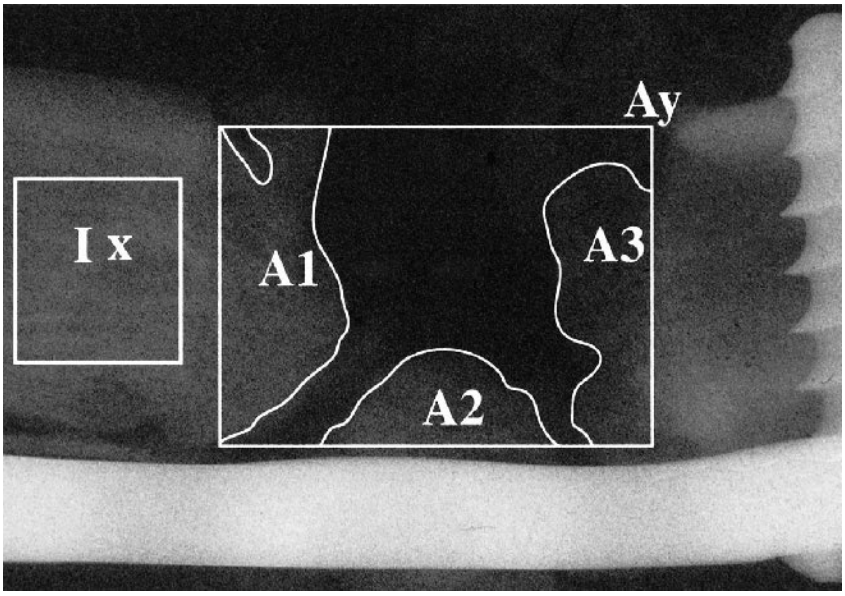

Fig 3 Measurement of bone formation index (BFI) using a ChemiImager 5500. A femur from the control group shows a small quantity of bone formed within the osteotomy gap at 8 weeks. Regions of measurement of area and radiopacity are delineated by black lines. Region Ay is the rectangular area representing the osteotomy gap area. Regions A1, A2, and A3 represent areas of bone within the gap, within which the average intensity is measured by the ChemiImager as a representation of radiopacity (and hence bone density). Ix is the intensity within the intracortical space of adjacent bone, which is used to calculate a relative radiopacity for the regions within the gap.

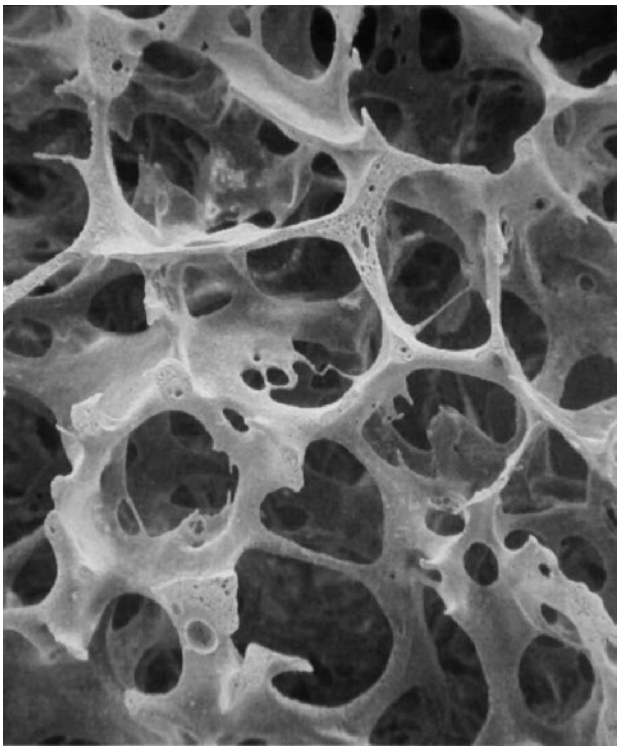

Fig 4 A scanning electron micrograph of the poly(lactide-*co*-glycolide) 75:25 scaffold.

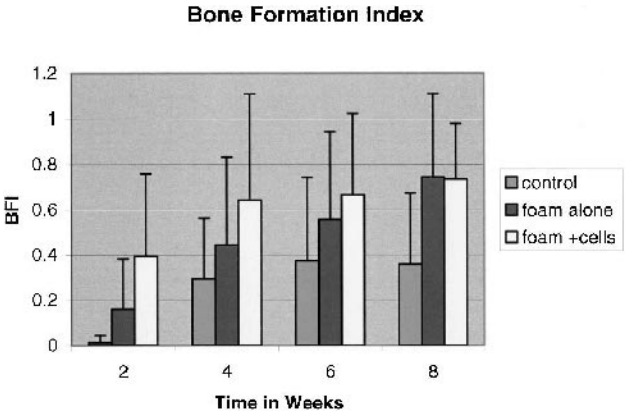

Fig 5 Bone formation index for all treatment groups over time. Means are significantly different at 2 and 8 weeks.

which was confirmed statistically with ANOVA ($P < 0.05$).

Finally, our results demonstrate that this plated femoral osteotomy model produced unexpected patterns of healing with a "neocortex" developing on the femoral side opposite to the fixation plate and resorption below the plate. The latter was seen to varying degrees in each treatment group and suggests the presence of stress shielding as a result of the plate, which may have ultimately affected the quantitative results. The development of a neocortex is more problematic, because it confounds union scores in this model. This exuberant new bone formation appeared initially as subperiosteal bone distal to the defect but grew parallel to the defect even though the periosteum had been stripped to a distance of 0.5 cm both proximal and distal to the defect. We believe that this was a tissue reaction to the changes in biomechanical environment wrought by the plated osteotomy site and that it has not been previously reported but would, in part, explain why others prefer

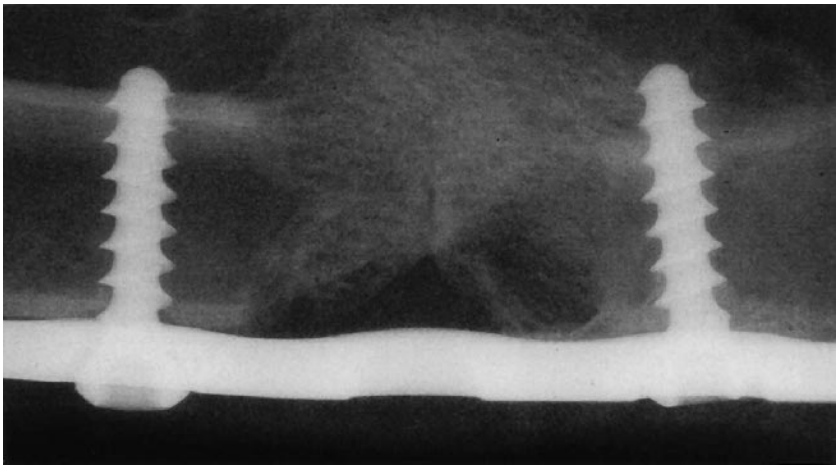

Fig 6 Radiograph of femoral osteotomy site in a cell-loaded group (III) rabbit showing significant filling of the osteotomy gap with bone in addition to the observed pattern of resorption adjacent to the plate (right = distal; bottom = lateral).

non-weight-bearing long bones such as the fibular or radius for investigations of healing in nonunion defects. This complication does not distract from the comparative differences seen between our three animal groups, however. Our results demonstrate that accelerated early healing of critical-sized segmental osteotomies in the rabbit femur can be achieved by combining autologous marrow cells with a novel macroporous biodegradable PLGA scaffold possessing an interconnecting macroporosity.

Further investigation is ongoing to confirm the efficacy of this cell-seeded scaffold technology as a means of engineering bone growth in the clinical setting.

This project was funded by grants from The Physicians' Services Incorporated Foundation (number 99-49 to J.A.F.) and from BoneTec Corporation and the Ontario Research and Development Challenge Fund (to J.E.D.).

References

1. Ito T, Sakano S, Sugiura H, et al. Sensitivity of osteoinductive activity of demineralized and defatted rat femur to temperature and duration of heating. Clin Orthop 1995;316:267–275
2. Salyer KE, Hall CD. Porous hydroxyapatite as an onlay bonegraft substitute for maxillofacial surgery. Plast Reconstr Surg 1995;84:236–244
3. Concannon MJ, Boschert MT, Puckett CL. Bone induction using demineralized bone in the rabbit femur: a long term study. Plast Reconstr Surg 1997;99:1983–1988
4. Salyer KE, Bardach J, Squier CA, et al. Cranioplasty in the growing canine skull using demineralized perforated bone. Plast Reconstr Surg 1995;96:770–779
5. Winn SR, Uludag H, Hollinger JO. Carrier systems for bone morphogenetic proteins. Clin Orthop 1999;367(Suppl):S95–106
6. Weinmann JP, Sicher H. Bone and Bones. 2nd ed. St. Louis: CV Mosby Company, 1955.
7. Ripamonti U. Smart biomaterials with intrinsic osteoinductivity: geometric control of bone differentiation. In: Davies JE (ed). Bone Engineering. Toronto: em squared Inc, 2000:215–222
8. Athanasiou KA, Agrawal CM (eds). Orthopedic polymeric biomaterials: applications of biodegradables. Biomaterials 2000;21(Suppl)
9. Davies JE (ed). Bone Engineering. Toronto: em squared Inc, 2000
10. Mooney DJ, Sano K, Kaufmann PM, et al. Long term engraftment of hepatocytes transplanted on biodegradable polymer sponges. J Biomed Mater Res 1997;37:413–420
11. Kim WS, Vacanti CA, Upton J, et al. Bone defect repair with tissue-engineered cartilage. Plast Reconstr Surg 1994;94:580–584
12. Kadiyala S, Jaiswal N, Bruder SP. Culture-expanded, bone marrow-derived mesenchymal stem cells can regenerate a critical sized segmental bone defect. Tissue Eng 1997;3:173–185
13. Bruder SP, Kurth AA, Shea M, et al. Bone regeneration by implantation of purified, culture-expanded human mesenchymal stem cells. J Orthop Res 1998;16:155–162
14. Niklason LE. Engineering of bone grafts. Nature Biotech 2000; 18:929–930
15. Vacanti CA, Bonassar LJ. An overview of tissue engineered bone. Clin Orthop 1999;367(Suppl):S375–381
16. Bruder SP, Fox BS. Tissue engineering of bone. Cell based strategies. Clin Orthop 1999;367(Suppl):S68–83
17. Fleming JE, Jr, Cornell CN, Muschler GF. Bone cells and matrices in orthopedic tissue engineering. Orthop Clin North Am 2000;31:357–374
18. Ohgushi H, Okumura M, Masuhara K, et al. Calcium phosphate block ceramic with bone marrow cells in a rat long bone defect. In: Yamamuro T, Hench LL, Wilson J (eds). CRC Handbook of Bioactive Ceramics, vol II. Boca Raton: CRC Press, 1992:235–238
19. Petite H, Viateau V, Bensaid W, et al. Tissue-engineered bone regeneration. Nat Biotech 2000;18:959–963
20. Ishaug-Riley SL, Crane GM, Gurlek A, et al. Ectopic bone formation by marrow stromal osteoblast transplantation using poly(DL-lactic-co-glycolic acid) foams implanted into the rat mesentery. J Biomed Mater Res 1997;36:1–8
21. Baksh D, Davies JE. Design strategies for 3-dimensional in vitro bone growth in tissue-engineering scaffolds. In: Davies JE (ed). Bone Engineering. Toronto: em squared Inc, 2000:488–495
22. Holy C E, Fialkov JA, Shoichet MS, et al. In vivo models for

bone tissue-engineering constructs. In: Davies JE (ed). Bone Engineering. Toronto: em squared Inc, 2000:496–504
23. Puelacher WC, Vacanti JP, Ferraro NF, et al. Femoral shaft reconstruction using tissue-engineered growth of bone. Int J Oral Maxillofac Surg 1996;25:223–228
24. Davies JE, Baksh D, Karp JM. Mesenchymal cell culture: bone. In: Atala A, Lanza R (eds). Methods in Tissue Engineering. San Diego: Academic Press, 2002:333–344
25. Rout PGJ, Tarrant SF, Frame JW, et al. Interactions between primary bone cell cultures and biomaterials. Part 3: a comparison of dense and macroporous hydroxyapatite. In: Pizzoferrato A, Ravaglioli PG, Lee AJC (eds). Biomaterials and Clinical Applications. Amsterdam: Elsevier, 1988:591–596
26. Yoshikawa T, Ohgushi H, Tamai S. Intermediate bone forming capability of prefabricated osteogenic hydroxyapatite. J Bio-Med Mater Res 1996;32:481–492
27. Holy CE, Shoichet MS, Davies JE. Bone marrow cell colonization of, and extracellular matrix expression on, biodegradable polymers. Cells Mater 1997;7:223–234
28. Holy CE, Davies JE, Shoichet MS. Bone tissue engineering on biodegradable polymers: preparation of a novel poly(lactide-*co*-glycolide) foam. In: Peppas NA, Mooney DJ, Mikos AG, et al (eds). Biomaterials, Carriers for Drug Delivery, and Scaffolds for Tissue Engineering. New York: AIChE Press, 1997:272–274
29. Baksh D, Davies JE, Kim S. Three dimensional matrices of calcium polyphosphates support bone growth in vitro and in vivo. J Mater Sci Mater Med 1998;9:743–748
30. LeGeros RZ, LeGeros JP. Calcium phosphate biomaterials: preparation, properties, and biodegradation. In: Wise DL, Trantolo DJ, Altobelli DE, et al (eds). Encyclopedic Handbook of Biomaterials and Bioengineering. Part A: Materials, vol 2. New York: Marcel Dekker, 1995:1429–1463
31. Holy CE, Fialkov JA, Davies JE, et al. Use of a biomimetic strategy to engineer bone. J Biomed Mater Res; in press
32. Holy CE, Dang SM, Davies JE, et al. In vitro degradation of a novel poly(lactide-co-glycolide) 75/25 foam. Biomaterials 1999;20:1177–1185
33. Inui K, Maeda M, Sano A, et al. Local application of basic fibroblast growth factor minipellet induces the healing of segmental bony defects in rabbits. Calcif Tissue Int 1998;63:490–495
34. Davies JE, Chernecky R, Lowenberg B, et al. Deposition and resorption of calcified matrix in vitro by rat marrow cells. Cells Mater 1991;1:3–15
35. Davies JE. In vitro modeling of the bone/implant interface. Anat Rec 1996;245:426–445